Sensors and Materials, Vol. 15, No. 6 (2003) 295–311
MYU Tokyo

S & M 0530

Integrated Fabrication of Polymeric Devices for Biological Applications

Mark J. Kastantin[1,2], Sheng Li[1,2], Anand P. Gadre[1,2], Li-Qun Wu[3,4], William E. Bentley[3,5], Gregory F. Payne[3,4], Gary W. Rubloff[2,6] and Reza Ghodssi[1,2]*

[1]Department of Electrical and Computer Engineering, University of Maryland (UMD) A.V. Williams Building, College Park, MD 20742, USA
[2]Inst. for Systems Research, UMD, A.V. Williams Building, College Park, MD 20742, USA
[3]Center for Biosystems Research, UMBI, College Park, MD 20742, USA
[4]Department of Chemical and Biochemical Engineering, UMBC, Baltimore, MD 21250, USA
[5]Dept. of Chemical Engineering, UMD, A.V. Williams Building, College Park, MD 20742, USA
[6]Dept. of Materials and Nuclear Engineering, UMD, A.V. Williams Building, College Park, MD 20742, USA

(Received May 8, 2003; accepted July 22, 2003)

Key words: integrative polymeric fabrication, SU-8, polypyrrole (PPy), polydimethylsiloxane (PDMS), chitosan, green fluorescent protein (GFP), bonding

A novel fabrication technique for all-polymeric, microfluidic bio-MEMS devices is presented. This device uses selective electrodeposition of a bio-polymer, chitosan, to successfully create an environment for complex biological experiments within an SU-8 microchannel. The surface energy between SU-8 and PDMS is measured to be 0.047 ± 0.018 J/m^2, allowing for reversible encapsulation of the microfluidic channel. The conducting material, polypyrrole, has a conductivity of 47 ± 5 S/cm and is explored as a replacement for metal electrodes in future work. It is the successful integration of these four polymers, however, that enables such versatile devices to be fabricated.

*Corresponding author, e-mail address: ghodssi@eng.umd.edu

1. Introduction

The use of micro-electro-mechanical systems (MEMS) in biological research is becoming increasingly common. Micro devices allow easier observation and manipulation of individual cells, proteins, or other biological macromolecules. Sample sizes for such experiments are also reduced when using MEMS as compared to traditional techniques.[1] This allows biological systems to be studied at a new level of resolution while minimizing the materials required for an experiment.

Initially, microfluidic devices were used primarily for capillary electrophoresis.[2–4] Recently, there has been interest in incorporating a complete array of functional units (valves, pumps, reaction chambers, etc.) onto a single chip to create a lab-on-a-chip (LOC).[5–11] These LOC units increase the range of experiments possible on the micro-scale.

A variety of methods are presently available for fabrication of microfluidic devices. Channels can be micromachined into silicon using traditional microelectronics techniques.[12–14] Glass can be a substrate for biological applications, allowing for visual observation of activity inside the channel.[15] However, glass and silicon processing are expensive and time-consuming. Often they require hazardous chemicals and expensive machinery. Polymeric methods provide a more flexible and cheaper alternative to the above techniques. Photolithographic-based processes create microchannels in polymeric materials such as polydimethylsiloxane (PDMS) or EPON SU-8 in a matter of hours. Processing these materials requires only a contact aligner for lithography and a few solvents.

Polymers provide a broad range of properties as structural and functional materials for development of MEMS devices. For instance, polymer functional groups provide an interface between the inert, structural aspects of a device and the biological components in a MEMS device. Rather than simply housing reactants, polymer properties can be tailored to provide an environment in which to sustain biological species.[16] Thus, the choice of polymers is crucial to the success of the device as each material adds its properties to the final environment for the experiment.

We investigate the use of chitosan, a biocompatible, biodegradable amino-polysaccharide biopolymer, to create an environment which will be biologically inert and flexible for sensing and manipulating macromolecules and organisms within a MEMS device.[17–19] The chitosan amine functional groups allow a wide array of biomacromolecules to be covalently coupled to chitosan for biological experiments such as biosensing. Furthermore, selective deposition of chitosan allows control over the spatial positioning of reactants.

Like many other biopolymers, chitosan is sensitive to the high temperatures and organic solvents traditionally used in MEMS fabrication. Consequently, the effective integration of cells and biological molecules into MEMS will likely require new microfabrication methods that can be performed in aqueous environments under ambient conditions. Our goal is to develop such techniques to lay the groundwork for development of next generation "polymeric only" devices for future drug delivery and LOC applications.

A new integrative polymeric fabrication method is presented in this paper for bioMEMS devices. The novel developmental aspects of this device are: 1) integration of four biocompatible polymers in one device, 2) a removable encapsulation method using spin-cast PDMS, 3) a macroscopic alignment method that is accurate on the micro-scale, 4) the use of polypyrrole (PPy) as a highly conducting polymer that can potentially replace thin film metals as functional electrodes in future work, and 5) the selective deposition of chitosan in the microchannels for ligand-coupling experiments.

The concepts presented in this work are also intended to be more generally applicable to creating MEMS devices for a variety of biological uses. Our techniques are modular, allowing one or two changes in mask design to adapt devices used for a specific application. For example, this work uses one inlet reservoir, one outlet reservoir, and one channel structure per device. It is not difficult to imagine a device with multiple inlet and outlet reservoirs and a complex channel structure. These changes would only require modification of the photolithographic masks for SU-8 and PDMS processing. The biologist or bioengineer can use these techniques in combination with previously developed packaging, pumping, and valving systems to tailor devices to a specific application.[5,11,20,21]

2. Materials and Methods

Materials of choice and fabrication methods are key aspects for developing bioMEMS devices. The four types of polymeric materials used in this work are chosen for their unique functional characteristics, integrative process properties and compatibilities. As shown in Fig. 1, PPy is used as the electrodes, which are covered by a two-level SU-8 structure. The first layer forms a channel as well as inlet and outlet reservoirs for fluid, while the second forms alignment posts for a PDMS encapsulation membrane. This system allows the channel to be covered while exposing reservoirs to the external environment for injection and removal of fluid. Chitosan is then selectively deposited on certain PPy electrodes located in the channel. By playing different roles, these polymers are integrated to create smart sensors and actuators for biological applications. The following sections describe the processing techniques, functions and characterization results for each polymer. The integrated device fabrication flow is also introduced in detail, including selective deposition of chitosan film within the encapsulated microfluidic channels.

2.1 *Polymeric materials*

2.1.1 *Structures in SU-8*

A two-level SU-8 formation is used as the main structure for this device. The first layer forms the structural material for the channel while the second layer is used to align the encapsulating PDMS layer. This alignment layer consists of four posts that align with holes in the PDMS layer. Thus, a pattern in the encapsulating layer can be aligned to the channel layer to create covered channels with open inlet and outlet zones. Furthermore, this procedure can be performed by hand as the PDMS cover will simply 'drop' onto the posts when positioned correctly using surface tension provided by drops of isopropanol.

In this process, SU-8, an epoxy resin, acts as a negative photoresist. When exposed to UV light, a Lewis acid catalyzes the hydroxyl coupling of the SU-8 epoxy rings, forming a

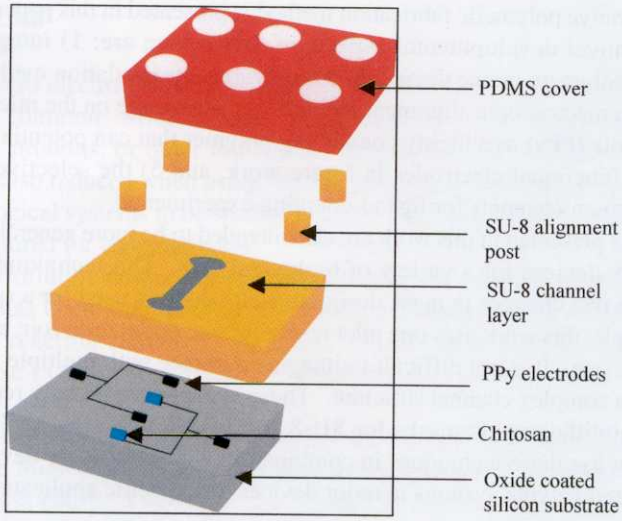

Fig. 1. Expanded view of the proposed device.

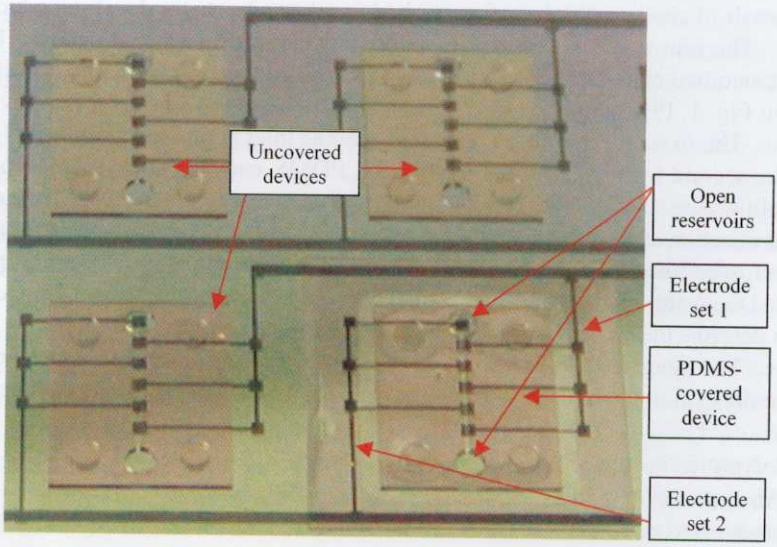

Fig. 6. Four completed devices are shown. Clear channel structures are seen as well as the alignment posts. PPy electrodes can also be seen running the length of the channel. One device is covered in PDMS (bottom right). The device is 4 mm wide by 5 mm long.

solid, cross-linked polymer matrix. SU-8 is useful for microfluidics because it can produce well-defined, high-aspect-ratio structures. Complex multi-layer surfaces can be created in this manner.[22–25]

SU-8 processing requires two baking steps. First, a pre-exposure bake helps to eliminate excess solvent from the photoresist matrix, increasing the resolution attainable with the negative photoresist. The post-exposure bake helps to complete the cross-linkage of the SU-8 chains, further solidifying the resulting structures. Unfortunately, SU-8 also has a high coefficient of thermal expansion, allowing excess heat to crack the cross-linked structure. This presents a problem for bilayer SU-8 structures because baking required for the second layer can crack the first layer. To combat this problem, the post-exposure bake for the first layer is used as a pre-exposure bake for the second layer. This reduces the total heat absorbed by the first layer and results in less cracking in the final structure.

2.1.2 *Encapsulation with polydimethylsiloxane*

The alignment system created by the two-level SU-8 structure described above allows not only for simple channel encapsulation, but also for easy removal of the covering. Because it is often undesirable to spend a long time fabricating devices for a particular experiment, the fabrication methods presented in this paper were designed to enable quick manufacturing of devices. Thus, removable encapsulation allows a wafer of devices to be cleaned and reused after an experiment. This convenience, however, introduces some limitations. For example, the covering is useful to prevent evaporation of aqueous solutions, but will not seal the channel against moderate or high pressure differentials.

The surface of PDMS can be oxidized by treatment with oxygen plasma. This creates -SiOH groups on the PDMS surface for adding other functional groups. Additionally, oxidized PDMS is hydrophilic and easier to use for microfluidics. When brought into contact with glass, silicon, quartz, silicon nitride, polyethylene, polystyrene, glassy carbon, or even other oxidized PDMS, an irreversible, covalent, siloxane bond is formed. Thus, channel encapsulation can be accomplished through this plasma oxidation.[26,27] Positive photoresists can also be used for wafer bonding and irreversible encapsulation of microchannels.[25,28]

Although polymeric components in this device are inexpensive, the time required to fabricate new devices makes reusable devices more attractive. Consequently, some applications may benefit from a removable encapsulation method. For removable coverings, covalent sealing techniques cannot be used. This limits the device in its capability to seal under higher pressures. However, the strength of the seal provided by the surface energy of PDMS is sufficient for most biological applications.

With these considerations in mind, a thin PDMS membrane is used as the encapsulation layer. PDMS is a tough elastomer that is relatively inexpensive and easy to work with. It is non-polar, impermeable to aqueous solutions, and can be molded against an SU-8 or silicon master to create the desired surface structures.[29] PDMS is typically poured onto a template so that it completely covers it. This results in patterning only on one side of the membrane. Holes are drilled in the PDMS to create inlet and outlet ports for microfluidic applications. Alternatively, large posts can be inserted into the mixture during curing and later removed to create ports.[5,26–28]

These methods afford only crude control over the resulting film thickness. However, PDMS thickness can be controlled by spin-casting that also allows patterning of both sides of the resulting PDMS layer in one step. If the thickness of the PDMS layer is less than that of the SU-8 master pattern, inlet and outlets are naturally created without the use of macroscopic fabrication techniques.

2.1.3 *Electrode formation with polypyrrole*

Electrodes are placed in a microfluidic device for several reasons. They are often used to record electrical activity from cells. Properly placed electrodes can record the activity from a single cell that rests on top of it.[30] Additionally, electrodes can be used for flow actuation. Some charged materials undergo conformational changes during an applied potential. Ferrofluids can also be attracted to an electrode, preventing fluid flow and acting as a valve.

PPy adds utility to current MEMS devices for use in biological experiments. Long-term compatibility of MEMS devices with mammalian cells is improved by using highly conducting polypyrrole instead of gold.[30] Furthermore, PPy can be easily deposited electrochemically due to aqueous solubility and low oxidation potential of the monomer.[20,31–33] Anionic doping of PPy enhances the conductivity as well as the hydrolytic stability of the film.[34]

While gold is commonly used for electrodes, polypyrrole is used in this device. In addition to enhancing survival in mammalian cell cultures (over gold), PPy is less expensive and easier to work with. While gold is typically deposited using e-beam evaporation to achieve a uniform layer, PPy can be solution cast or electrodeposited. While this work uses gold as a base layer for PPy electrodeposition, it is possible to pattern self-assembled conducting polymer bilayers on bare silicon.[35] Using these techniques, the use of gold can be circumvented.

2.1.4 *Device functionality through selective chitosan deposition*

Often, it is desirable to anchor cells, proteins, or other molecules to the channel bottom. For example, if a large number of experiments are to be performed on the same type of cell or protein, it might make sense to anchor the cell to the channel and pass different reactants over it. Furthermore, in order to make accurate measurements of electrical activity within the cells, they must be in close proximity to the recording electrodes. Thus, chitosan is used in this work to effectively 'glue' biological samples to specific locations in the channel.

Selective deposition of chitosan is also demonstrated in this work. This affords some control over the number of substrates that can be held in the channel simply by controlling the chitosan deposition area. In experiments where reactant stoichoimetry is important, such control is critical to success. Furthermore, this deposition allows some electrodes to be designated as sensing electrodes that hold reactants and record electrical activity. Other electrodes, free of reactants, can act as actuating electrodes for flow control.

Chitosan is an amino-polysaccharide that is water-soluble at low pH.[36,37] At higher pH (> 6.3), the amino group becomes deprotonated and the polymer precipitates out of solution. Chitosan can therefore be deposited from an aqueous solution under mildly acidic conditions. If a negative charge is induced on an electrode, deposition has been shown to occur on that electrode.[17–19] Thus, chitosan selectively electrodeposits on cathodes while deposition fails to occur on unpolarized or positively charged surfaces. From a processing standpoint, its pH-dependent solubility makes chitosan an attractive polymer to use in a MEMS device.

The primary amine groups present in chitosan can be used not only as the mechanism of deposition, but also to chemically modify the surface properties of chitosan. Unlike other biopolymers such as polylysine, it is chemically reactive to amine group chemistries in a broad range of pH environments. High pH is required to deprotonate the amine groups of polylysine (>10.5), whereas chitosan is nucleophilic above a pH of 6.3. The nucleophilic properties of the amine group allow it to react with other molecules, including proteins, oligonucleotides, and even cells.

It is this property of chitosan that makes our device so versatile while still allowing simple fabrication. Conventional coupling methods for anchoring biomolecules, such as silanization, require laborious, hard-to-control and non-selective steps on inorganic surfaces.[38,39] In contrast, a mild, non-disruptive reaction environment can be created using chitosan, preserving biological activities and selectivities. This ability to easily anchor proteins to the MEMS device allows it to be used for biosensing applications by studying antigen-antibody interactions.

2.1.5 *Use of green fluorescent protein (GFP) to demonstrate protein assembly onto the selectively deposited chitosan*

Green fluorescent protein (GFP) is a convenient model because the intact protein can be readily visualized under UV illumination.

Prepared by well-established bioengineering methods, GFP was expressed in E.coli BL21 (Invitrogen) using a pTrcHisB (Invitrogen) expression vector. Cells were grown under standard fermentation conditions and the fusion protein was purified using immobilized metal affinity chromatography as described elsewhere.[40,41]

Glutaraldehyde was used to anchor the model protein, GFP, onto the selectively deposited chitosan on the PPy electrodes. After chitosan was selectively deposited, the wafer was immersed in glutaraldehyde solution (0.05%) for 30 min. After glutaraldehyde activation, the wafer was extensively washed with 0.1 M PBS (Dulbecco's Phosphate Buffered Saline, Sigma-Aldrich Chemicals) buffer and then immersed in a GFP solution (≈ 0.4 mg/ml) for 30 min. Two control experiments were performed at the same time. One control was a wafer with devices that lacked chitosan. The second control was a wafer in which chitosan was deposited onto the channel's electrodes, but the deposited chitosan was not activated with glutaraldehyde. Both controls were immersed in GFP solution for 30 min. All samples were extensively washed with PBS buffer before examination.

The bio-functionalized microfluidic channels were examined using a fluorescence stereomicroscope (MZFLIII, Leica) with a fluorescence filter set (GFP Plus) using an excitation filter at 480 nm (band width of 40 nm) and an emission barrier filter at 510 nm. Photomicrographs were prepared from the fluorescence microscope using a digital camera (Spot 32, Diagnostic Instruments).

2.2 *Materials characterization*

Physical properties of two polymers used in this work, PPy and PDMS, are particularly critical to the operation of the device. As a functional material, it is essential for the deposited PPy film to have relatively high conductivity. For channel encapsulation, it is necessary to have sufficient surface energy at the interface of PDMS and SU-8. This

section assesses the performance of these two materials in the device.

Test structures were designed and fabricated for measuring the conductivity of the PPy film. First, one layer of chromium (30 Å thick) was deposited on a silicon wafer coated with 1-μm-thick thermal SiO_2, followed by evaporating a layer of gold (2000 Å thick). Photoresist was spun and patterned on the top of gold using the mask pattern shown in Fig. 2(a). Au and Cr layers were patterned with wet chemical etching using gold and chromium etchants, respectively to form a 40-μm-wide serpentine trench. PPy was then electrochemically deposited from a solution of 0.1 M pyrrole (Aldrich) and 0.1 M NaDBS (Aldrich) in the trench as shown in Fig. 2(b). Thickness and resistance of the PPy film deposited in the trench were measured using a profilometer and a probe station, respectively.

The thickness of the PPy film is plotted as a function of deposition time in Fig. 3 at the constant applied potential of 0.55 V (vs. an Ag/AgCl reference electrode).[42,43] These data show that film growth is linear. Thus, as long as a constant concentration of monomer is maintained in the aqueous solution, the rate of film growth should be constant at that voltage.

Electrical conductivity of the PPy film was then calculated as the inverse of the resistivity of the sample using the following equation:

$$\sigma = \frac{1}{\rho} = \frac{L}{RS} \tag{1}$$

where σ, ρ, R, L and S are the conductivity, resistivity, resistance, length and cross section area of the PPy film filled in the trench, respectively. The average conductivity of PPy film was determined to be 47 $\pm$ 5 S/cm. This is higher than the 8.3 S/cm reported by Omastova

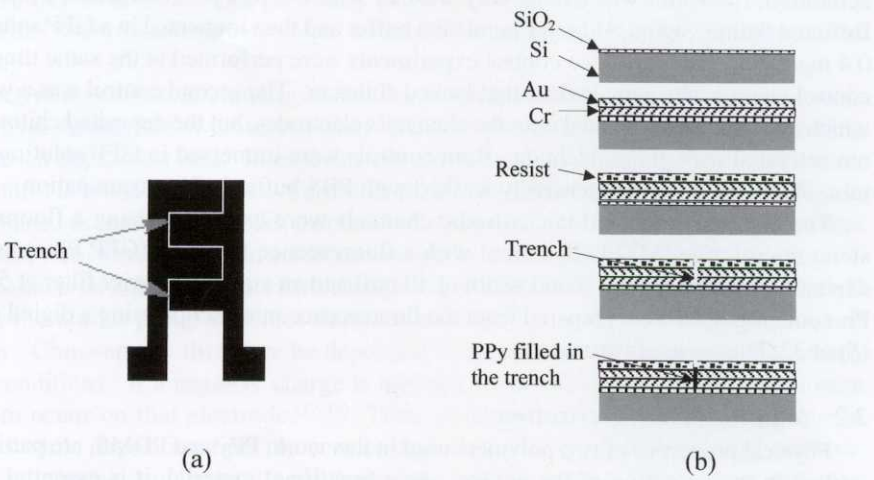

Fig. 2. The mask pattern (a) and process flow (b) used in the experiment for measuring the conductivity of PPy film.

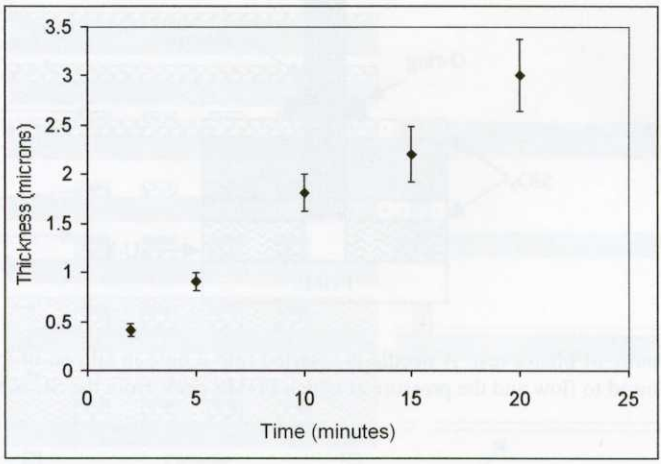

Fig. 3. Deposition of polypyrrole on gold electrodes. The thickness of PPy is shown as a function of deposition time for monomer concentrations of 0.1 M and 0.55 V (vs. Ag/AgCl). The linear relationship allows for a controlled deposition depending on desired conductivity. Error bars reflect one standard deviation in each measurement.

et al. for NaDBS doped PPy films, but well within the range proposed by Gardner and Bartlett (10^{-5}–10^{2} S/cm) for PPy films in general.[31,34] The discrepancy is attributed to different preparation methods, doping levels, and evaluation techniques used for PPy films.

The bond strength between SU-8 and PDMS is critical for proper sealing of the device. Because the encapsulation is reversible, low bond strength is expected. Still, the encapsulation should be strong enough to prevent water leakage during a typical experiment. An estimate of the bond strength between PDMS and SU-8 was made using the 'blister test'.[44,45] For this test, a tunnel was created in a silicon wafer. Thermal oxide (SiO_2) was first deposited on both sides of the wafer. Next, photoresist was spun on both SiO_2 layers. The backside resist layer was patterned and developed, followed by etching the oxide layer with buffered HF. The combination of resist and oxide was used as the mask for deep reactive ion etching circular holes in the silicon substrate. Subsequently, a 10-μm-thick SU-8 layer was deposited and patterned on the membranes and other oxide areas to create holes in SU-8. The SiO_2 membranes were etched away with reactive ion etching, leaving a cylindrical tunnel through the multi-layer structure.

As shown in Fig. 4, pressure was applied on the PDMS covering by flowing nitrogen gas (N_2) through a needle into the tunnel. The O-ring was used to prevent the leaking of N_2. The pressure was increased from atmospheric pressure at a rate of 20 Torr/min until the PDMS was observed to peel off from the SU-8, creating a blister. The resulting surface energy was calculated using the formula:[44,45]

$$\gamma = \frac{0.088 P_f^2 a^4}{E t_w^3} \tag{2}$$

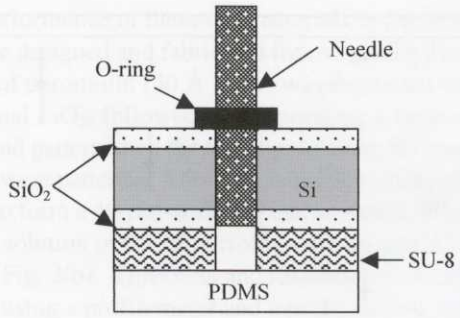

Fig. 4. Schematic of blister test. A needle is inserted into a hole in silicon of known diameter. Nitrogen is allowed to flow and the pressure at which PDMS peels from the SU-8 is recorded.

in which P_f is the critical pressure for debonding, a is the radius of the hole, E is Young's modulus of PDMS (7.5×10^5 Pa) and t_w is the thickness of PDMS.

With a 70-μm-thick PDMS cover on a hole of radius 300 μm, the critical pressure for debonding was found to be 30.7 Torr above atmospheric pressure. Thus, the surface energy was calculated to be 0.047 ± 0.018 J/m^2. This value is comparable with the values obtained for bonded hydrophilic silicon wafers. It is typical of surfaces bonded by Van der Waals forces in combination with weak chemical interactions (*e.g.*, relatively weak hydrogen bonds).[46] This surface energy is sufficient to prevent water leakage from the microfluidic channel of the device at the low pressures typically encountered during a biological experiment.

2.3 *Device fabrication*

The fabrication of the device starts with deposition and patterning of two layers of chromium and gold to form the electrodes. PPy is then deposited on the top of these electrodes. A two-layer SU-8 structure covers the PPy electrodes. Chitosan is then selectively deposited on certain areas of the channel bottom. The detailed process flow for fabricating this device is explained in the following paragraphs and shown in Fig. 5.

The first step in the fabrication was the deposition of a chromium adhesion layer on a silicon wafer coated with 1-μm-thick thermal SiO_2. Chromium was deposited using e-beam evaporation, to a thickness of 90 Å. Gold was evaporated immediately afterward to a thickness of 2000 Å.

Electrodes were then patterned using photolithography. A transparency mask was used to pattern a protective layer of photoresist (Shipley 1813) over the gold. Wet chemical etching was used to pattern the Au and Cr layers.

The wafer was then cleaned with piranha solution (3:1 ratio of H_2SO_4:H_2O_2) as a preparation for PPy deposition. PPy was then deposited electrochemically from an aqueous solution of 0.1 M pyrrole and 0.1 M sodium dodecyl benzene sulphonate (NaDBS).[42,43] A constant potential of 0.55 V (versus Ag/AgCl) was applied until a thickness of approximately 1–3 μm was reached.

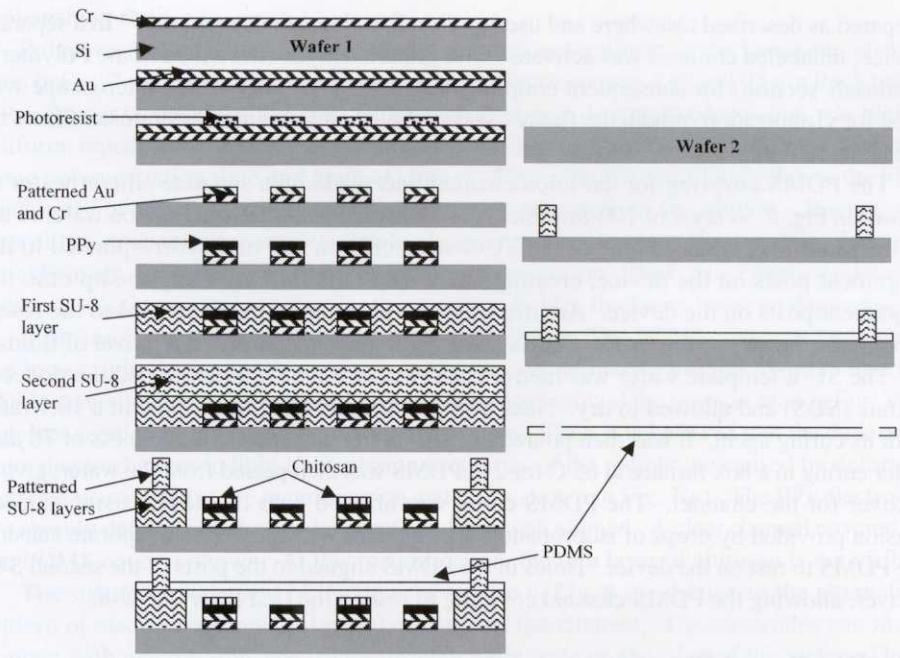

Fig. 5. Fabrication process flow for the device. On wafer 1, electrodes are first patterned, then a two-layer SU-8 structure is created. Chitosan is then deposited along with the PDMS cover to complete the device. The SiO_2 layer, part of the substrate, is not shown in this view. On wafer 2, the PDMS cover is patterned and removed for use on wafer 1.

Microfluidic channels were then constructed on top of the PPy electrodes using soft lithographic techniques. The first layer of SU-8 was spun to a thickness of 100 μm, baked, and exposed to create the reservoirs and channels. A second, 100-μm-thick layer of SU-8 was spun on top of the first layer. The post-bake step for the first layer served as the pre-bake step for the second layer. The second layer was then exposed to create the alignment posts for the PDMS cover. After baking and development, a clear, two-layer SU-8 structure remained.

After SU-8 processing, the biopolymer (either chitosan or a fluorescently-labeled chitosan derivative) was electrodeposited on PPy from a 0.6 wt % solution with an applied current density of 1–2 A/m^2 for 15 min. In this step, the wafer coated with PPy was immersed in solutions containing either fluorescently-labeled chitosan or unlabeled chitosan. As shown in Fig. 6, there are two sets of electrodes placed alternately in each device channel. 'Electrode set 1' was polarized to serve as the cathode while 'electrode set 2' was not polarized. Therefore, selective deposition of chitosan could be realized. The anode used for the electrodepostion was an unpatterned silicon wafer coated with 90-Å-thick Cr and 2000-Å-thick Au. Both the anode and cathode were connected to a potentiostat (model 363 PerkinElmer Instruments) with alligator clamps. When chitosan deposition was finished, the device was washed with DI water and dried. A solution of NaOH (1 M) was used to neutralize chitosan for 30 min. In one device, fluorescently-labeled chitosan was

prepared as described elsewhere and used to visualize chitosan deposition.[17] In a separate device, unlabeled chitosan was activated with glutaraldehyde (described in the Polymeric Materials section) for subsequent coupling with GFP. A fluorescence microscope was used for visualization of both the fluorescently-labeled chitosan and the chitosan film with the tethered GFP.

The PDMS covering for the microchannel was made on a separate silicon wafer as shown in Fig. 5. A layer of 100-μm-thick SU-8 was first patterned on a silicon wafer to act as the mold for PDMS. Some of the SU-8 structures on this mold corresponded to the alignment posts on the device, creating holes for the PDMS covering to slip onto the alignment posts on the device. Additionally, two other posts corresponded to the reservoirs, creating an opening in the PDMS covering for the injection and removal of fluids.

The SU-8 template wafer was then washed with a 0.1 M solution of sodium dodecyl sulfate (SDS) and allowed to dry. Next, PDMS (Sylgard 184) was mixed in a 10:1 ratio with its curing agent. It was then poured onto the wafer and spun to a thickness of 70 μm. After curing in a box furnace at 65°C for 2 h, PDMS was then peeled from the wafer, giving a cover for the channel. The PDMS cover was aligned onto the device using surface tension provided by drops of isopropanol. The alcohol was allowed to evaporate causing the PDMS to rest on the device. Holes in the PDMS aligned to the posts of the second SU-8 layer, allowing the PDMS channel covering to rest on the first layer of SU-8.

3. Results and Discussion

This technique successfully created a microfluidic device using integrative polymeric materials on a silicon substrate coated with silicon dioxide. A simple method was constructed to encapsulate the microchannel and allow subsequent removal of the PDMS encapsulating cover. Furthermore, alignment of the covering with the reservoirs was performed manually using the alignment posts. The results of this can be seen in Fig. 7. The large circle to the left is the alignment post while the one to the right is the reservoir. The PDMS covering is clear in both pictures, but appears dark in some areas of Fig. 7(a). In this area, the PDMS is stressed by the SU-8 alignment post, which is slightly larger in diameter than the opening in the PDMS. This changes the shape of the flat PDMS membrane in the stressed areas. It is believed that this change alters the way that light is transmitted through the membrane, creating the darkness seen under the optical microscope. To avoid this problem, holes should be created in PDMS that are larger than the SU-8 alignment posts. This darkness disappears in Fig. 7(b) when the magnification and focus is changed. PDMS appears over the covered channel as a clear film in Fig. 7(b). It is also apparent that this alignment was highly accurate as the PDMS covering closely follows the curvature of the SU-8 reservoir.

This simple alignment method is reversible so that the cover can be removed, allowing the device to be cleaned and reused. The surface energy is sufficiently high to prevent leakage of aqueous fluids at the low pressures necessary for biological applications. Furthermore, because PDMS is impermeable to aqueous solvents, the surface area for evaporation is reduced to only the channel ends, rather than the top of the channel. This allows a controlled environment to be maintained in the channel with a minimal amount of

replenishing fluid.

Polypyrrole electrodes that are sharply defined and uniform in thickness can also be seen in Fig. 7. The PPy film was measured to be approximately 1.89 ± 0.03 μm thick using a P-1 Tencor contact profilometer. While film thickness during one deposition was highly uniform, repeatability between depositions could vary by as much as 0.5 microns given the same polymerization time and applied voltage. This effect is most likely due to the high sensitivity of the deposition rate on monomer concentration in solution. During one deposition, concentration remains relatively constant, but because the monomer degrades quickly in air, the solution is made fresh for each deposition. Thus, concentration variation between solutions could account for the variation in film thickness between depositions.

A picture of the completed device is shown in Fig. 6. The PDMS cover can be seen on the lower right device while an uncovered device is shown on the left. Notice that the PDMS covering does not appear to have the dark rings around the posts as seen in Fig. 7(a), but does seem to be slightly deformed in those areas. Thus, it is believed that the dark rings were due to changes in light transmission properties of the membrane caused by deformation that was visible at the magnification and focus shown in Fig. 7(a). The PPy electrodes are sharply defined and the two levels of SU-8 are well aligned. A clear channel covered by the PDMS cover is shown. At this magnification, the thin layer of chitosan is not visible.

The spatial arrangement of the devices is seen in Fig. 6 in addition to the alternating pattern of electrodes running down the length of the channel. The electrodes can make contact with macroscopic electrodes through large pads on the edge of the wafer. These pads are connected to the devices through the wide lines of PPy running from left to right through the rows of devices. The shape and spatial arrangement of devices can be changed in the mask design to suit the needs of a particular experiment. Furthermore, the number and pattern of electrodes can be modified to achieve the desired arrangement of sensors and actuators throughout the device. The selective deposition of chitosan is also affected by this stage of mask design.

Fluorescently-labeled chitosan was deposited selectively on the PPy electrodes in the channel as seen in Fig. 8. The electrodes to which the negative potential was applied have a layer of fluorescently-labeled chitosan on them while the other electrodes do not. This is seen as a rainbow color on the electrodes in the optical picture and can be compared to the fluorescently tagged pattern when a fluorescent microscope was used. This comparison confirms that the film seen in Fig. 8(a) is labeled-chitosan. Film thickness was measured to be 1.03 ± 0.05 μm.

Glutaraldehyde is a homo-bifunctional coupling agent that reacts with amines and is commonly used for coupling biopolymers (*e.g.* proteins and nucleic acids). In previous work, amine-terminated oligonucleotide probes were coupled to the glutaraldehyde-activated chitosan surface.[47] This approach can be used to create biosensors based on nucleic acids. Glutaraldehdye can also be used to couple proteins to chitosan, although proteins are considerably more labile than nucleic acids. To examine protein coupling, we used the common model protein, green fluorescent protein (GFP). After depositing chitosan onto the patterned gold surface on the bottom of devices, the chitosan was activated with glutaraldehyde, extensively washed with buffer, and then contacted with a GFP-containing solution. Figure 9 shows that GFP is selectively coupled to the chitosan film that had been templated onto the microfluidic channels. As described in the "Materials and Methods"

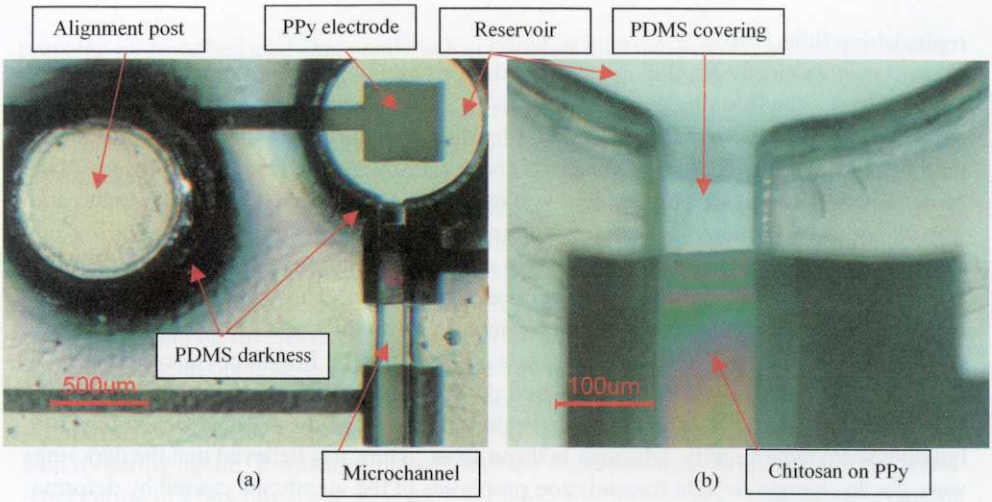

Fig. 7.

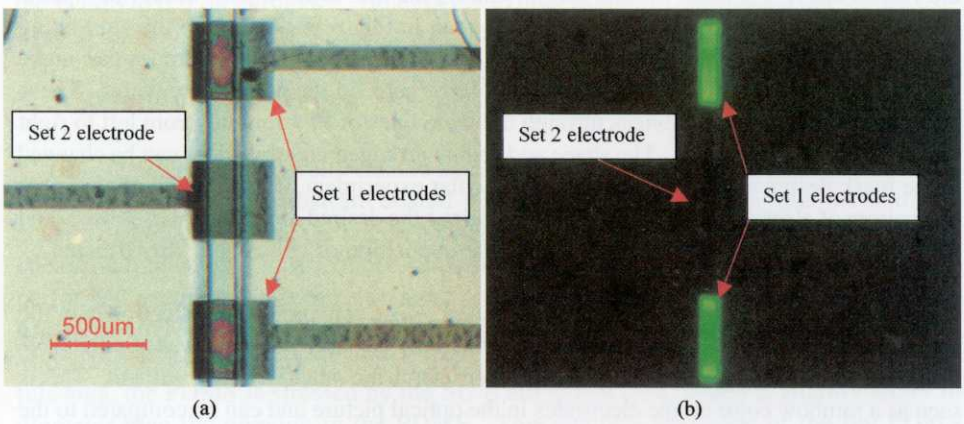

Fig. 8.

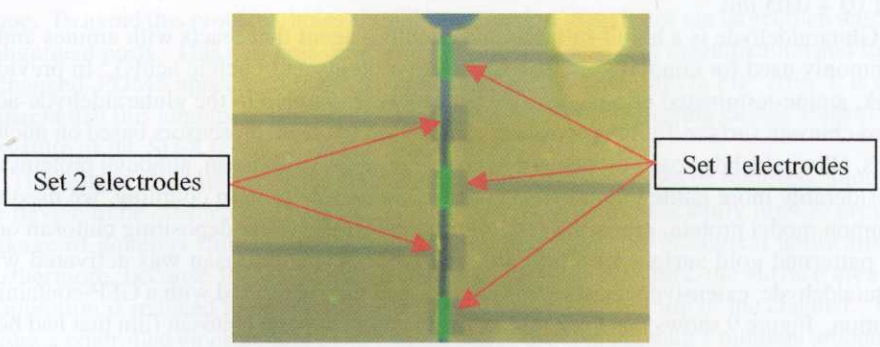

Fig. 9.

Fig. 7 (top). Microchannel encapsulation with PDMS. (a) A cover of PDMS lies on top of the SU-8 channel structure. An alignment post can be seen (left) in addition to the uncovered reservoir. Dark areas are believed to represent deformities in PDMS that change its light transmission properties. This phenomenon is only apparent at certain magnifications as the darkness around the reservoir disappears in (b). (b) Close up of the channel opening shows satisfactory alignment of PDMS and SU-8 without the darkness seen in (a).

Fig. 8 (middle). Selective deposition of fluorescently-labeled chitosan. (a) Fluorescently-labeled chitosan can be seen on set 1 electrodes. Deposition on the negative electrodes (set 1) only occurred in the channel areas, i.e., where the electrodes were uncovered by SU-8. No deposition was observed on the positive electrode in the middle (set 2). (b) The same area was observed with a fluorescence microscope. Areas showing fluorescently-labeled chitosan align with the rainbow-colored areas seen in (a).

Fig. 9 (bottom). Bio-functionalization of the device. Model protein (GFP, green fluorescent protein) was coupled to chitosan (on set 1 electrodes) that had been templated onto the microfluidic channels. Standard glutaraldehyde-based chemistry was used to activate chitosan surfaces for subsequent protein coupling.

section, two control experiments were performed: one in which chitosan was not deposited and a second in which chitosan was deposited but not activated with glutaraldehyde. No fluorescence was observed in either control. Thus, GFP was successfully patterned in the microchannel, opening the door for the coupling of other proteins, such as enzymes and antibodies relevant to biosensing and other biological applications.

4. Conclusions

Four polymers, commonly used separately, were successfully integrated in this work. Selective deposition of chitosan and polypyrrole was shown to be compatible with the processing of the other structural polymers in the device. PDMS was spin-cast on an SU-8 master to create an alignment system as well as inlet and outlet ports. The alignment system was easily manipulated by hand, and reversibly bonded to SU-8 with a surface energy of 0.047 ± 0.018 J/m^2. Additionally, conductivity measurements showed that polypyrrole (47 ± 5 S/cm) can be used as an inexpensive alternative to gold that is more compatible with biological applications. Solution casting of polypyrrole can replace the electrodeposition step in future work, thus eliminating the use of gold altogether.

Chitosan was used to couple a model protein, GFP, to the bottom of the channel, allowing the properties of biomacromolecules to be studied at high resolution in our MEMS device. Furthermore, the selective deposition of chitosan allows the scientist to control spatial aspects of an experiment.

The four biocompatible polymers integrated in this work can be used by the biologist to design micro-scale experiments by simply changing the mask design for the various polymer layers. This modular process is also relatively inexpensive due to its polymeric components. The range of experiments possible using biocompatible MEMS is consequently expanded.

Acknowledgements

This research is supported by the Small Smart Systems Center (SSSC) at University of Maryland (UMD). The authors would like to thank Professor Elisabeth Smela of the Department of Mechanical Engineering at UMD for her helpful discussions with the characterization of PPy films. Also, our gratitude is given to Mr. Nolan Ballew and Mr. Tom Loughran for their assistance in using the cleanroom facilities at UMD.

References

1 J. D. Trumbull, I. K. Glasgow, D. J. Beebe and R. L. Magin: IEEE Transactions on Biomed. Eng. **47** (2000) 3.
2 S. Jacobson, R. Hergenroder, L. Koutny and J.M. Ramsey: Anal. Chem. **66** (1994) 1114.
3 D. J. Harrison, A. Manz, Z. Fan, H. Luedi and H. M. Widmer: Anal. Chem. **64** (1992) 1926.
4 Z. Liang, N. Chiem, G. Ocvirk, T. Tang, K. Fluri and D. J. Harrison: Anal. Chem. **68** (1996) 1040.
5 J. Voldman, M. Gray and M. Schmidt: J. Microelectromech. Sys. **9** (2000) 295.
6 I. Glasgow, H. Zeringue, D. Beebe, S.-J. Choi, J. Lyman, N. Chan and M. Wheeler: IEEE Transactions on Biomed. Eng. **48** (2001) 570.
7 T. Fujii: Microelectronic Eng. **61–62** (2002) 907.
8 A. Yamaguchi, P. Jin, H. Tsuchiyama, T. Masuda, K. Sun, S. Matuso and H. Misawa: Analytica Chimica Acta. **468** (2002) 143.
9 J.-H. Kim, B.-G. Kim, J.-B. Yoon, E. Yoon and C.-H. Han: Sensors and Actuators A **95** (2002) 108.
10 M. Krishnan, V. Namasivayam, R. Lin, R. Pal and M. Burns: Curr. Opinion Biotech. **12** (2001) 92.
11 A. Hatch, A. Kamholz, G. Holman, P. Yager and K. Bohringer: J. Microelectromech. Sys. **10** (2002) 215.
12 M. de Boer, R. Tjerkstra, J. W. Berenschot, H. Jansen, G. J. Burger, J. G. E. Gardeniers, M. Elwenspoek and A. van den Berg: J. Microelectromech. Sys. **9** (2000) 94.
13 G. Kovacs, N. Maluf and K. Petersen: Proc. IEEE. **86** (1998) p. 1536.
14 J. Bustillo, R. Howe and R. Muller: Proc. IEEE. **86** (1998) p. 1552.
15 C.-H. Lin, G.-B. Lee, Y.-H. Lin and G.-L. Chang: J. Micromech. Microeng. **11** (2001) 726.
16 Y.-C. Wang, S.-H. Kao and H.-J. Hseih: Biomacromolecules. **4** (2003) 224.
17 L.-Q. Wu, H. Yi, S. Li, G. Rubloff, W. Bentley, R. Ghodssi and G. Payne: Langmuir. **19** (2003) 519.
18 L.-Q. Wu, A. Gadre, H. Yi, M. Kastantin, G. Rubloff, W. Bentley, G. Payne and R. Ghodssi: Langmuir. **18** (2002) 8620.
19 R. Fernandes, L.-W. Wu, T. Chen, H. Yi, G. W. Rubloff, R. Ghodssi, W. E. Bentley and G.F. Payne: Langmuir. **19** (2003) 4058.
20 E. Smela and J. Micromech: Microeng. **9** (1999) 1.
21 J.-H. Tsai and L. Lin: J. Micromech. Microeng. **11** (2001) 577.
22 J. Zhang, K.L. Tan, G. D. Hong, L .J. Yang and H. Q. Gong: J. Micromech. Microeng. **11** (2001) 20.
23 J. Zhang, K. L. Tan and H. Q. Gong: Polymer Testing. **20** (2001) 693.
24 R. Jackman, T. Floyd, R. Ghodssi, M. Schmidt and K. Jensen: J. Micromech. Microeng. **11** (2001) 263.

25 C.-T. Pan, H. Yang, S.-C. Shen, M.-C. Chou and H.-P. Chou. J. Micromech. Microeng. **12** (2002) 611.
26 D. Duffy, O. Schueller, S. Brittain and G. Whitesides: J. Micromech. Microeng. **9** (1999) 211.
27 D. Duffy, J. C. McDonald, O. Schueller and G. Whitesides: Anal. Chem. **70** (1998) 4974.
28 B.-H. Jo, L. van Lerberghe, K. Motesgood and D. Beebe: J. of Microelectromech. Sys. **9** (2000) 76.
29 J. O'Brien, P.J. Hughes, M. Brunet, B. O'Neill, J. Alderman, B. Lane, A. O'Riordan and C. O'Driscoll: J. Micromech. Microeng. **11** (2001) 353.
30 X. Cui, J. Hetke, J. Wiler, D. Anderson and D. Martin: Sensors and Actuators A **93** (2001) 8.
31 J. Gardner and P. Bartlett: Sensors and Actuators A. **51** (1995) 57.
32 M. Bazzaoui, L. Martins, E. A. Bazzaoui and J. I. Martins: Electrochimica Acta. **47** (2002) 2953.
33 M. L. Renak, G. C. Bazan and D. Roitman: Adv. Mat. **9** (1997) 392.
34 M. Omastova, M. Trchova, J. Kovarova and J. Stejskal: Synthetic Metals. In Press (2003).
35 X. Jiang and P. Hammond: Langmuir. **17** (2001) 8501.
36 P. Sorlier, A. Denuziere, C. Viton and A. Domard: Biomacromolecules. **2** (2001) 765.
37 F. Ligler, B. Lingerfelt, R. Price and P. Schoen: Langmuir. **17** (2001) 5082.
38 T. Sato, D.G. Hasko and H. Ahmed: Journal of Vac. Sci. Technol. B **15** (1997) 45.
39 J. Wang, T. Zhu, J. Song and Z. Liu: Thin Solid Films. **327** (1998) 591.
40 H. J. Cha, N. G. Dalal, M. Q. Pham and W. Bentley: Biotechnology Progress. **15** (1999) 283.
41 H. J. Cha, C.-F. Wu, J. J. Valdes, G. Rao and W. Bentley: Biotechnol. and Bioeng. **67** (2000) 565.
42 S. Li, E. Smela and R. Ghodssi: AVS 48th International Symposium (2001).
43 A. Gadre, M. Kastantin, S. Li and R. Ghodssi: Proc. ISDRS (2001) p. 186.
44 Q.-Y. Tong and U. Gösele: Semiconductor Wafer Bonding, (Wiley, New York, 1999) Chap. 2.
45 M. L. Williams: Journal of Applied Polymer Science **13** (1969) 29.
46 R. Stengl, T. Tan and U. Gösele, Jpn: J. Appl. Phys. **28** (1989) 1753.
47 H. Yi, L.-Q. Wu, J. Sumner, J. Gillespie, G. Payne and W. Bentley: Biotechnol. and Bioeng. In Press (2003).